Jahn-Teller spin polarons in perovskite cobaltites

D. Phelan,[*] J. Yu, and Despina Louca

Department of Physics, University of Virginia, Charlottesville, Virginia 22904, USA

(Received 7 May 2008; revised manuscript received 16 July 2008; published 19 September 2008)

The interplay of the electron transfer integral and lattice elastic energy in $A_{1-x}A'_x CoO_3$ is investigated by neutron diffraction and the pair density function analysis. By effectively widening the bandwidth with Ca, Sr, and Ba substitutions at the A site, evidence for the stability of the intermediate-spin (IS) configuration through the formation of static local Jahn-Teller (JT) distortions is provided. When the critical radius exceeds ~ 1.22 Å, spin activated JT polarons are formed in the absence of long-range magnetic ordering. JT polarons are prevalent in crystals with Sr and Ba but not in those with Ca. In the metallic and magnetically ordered phase, the static signature of the distortions is absent, suggesting that the IS state may be dynamically shared between Co^{3+} and Co^{4+} ions.

The complex nature of the spin, charge, and lattice interactions in some perovskite oxide crystals often yields unusual magnetoelastic and electron-phonon mechanisms, influenced by extrinsic and intrinsic parameters.[1–7] Take the perovskite cobaltite for example, $A_{1-x}A'_x CoO_3$ (A=trivalent rare-earth ion and A'=divalent alkaline-earth ion): the parent compound, $ACoO_3$, is a nonmagnetic ($S=0$) insulator that can be made ferromagnetic (FM) and conductive through the substitution of A' for A.[8–10] The evolution from a nonmagnetic to a static FM ground state is not obvious at first sight since all $3d^6$ electrons of the octahedrally coordinated Co^{3+} reside in the low-lying t_{2g}^6 orbitals with the low-spin (LS) configuration.[11–15] This implies that the Co^{3+} and/or the Co^{4+} ions created by the addition of holes become magnetically active. Indirect exchange interactions via t_{2g} orbitals are anticipated to be weak, while superexchange or double exchange (DE) interactions[16] via e_g orbitals dominate the magnetic coupling. The FM transition is usually attributed to the DE mechanism that involves spins excited to the e_g level in either the $S=1$ intermediate-spin (IS) or the $S=2$ high-spin (HS) state involving either Co^{3+} or Co^{4+} ions or both. Several possible scenarios can be considered to account for the magnetic coupling and this has been a subject of debate.[17,18] Many attempts have been made to distinguish the LS, IS, and HS configurations in the parent compound (with no Co^{4+}) by focusing on structural signatures. The problem is made even harder when Co^{4+} ions are introduced in the lattice.

Our earlier neutron measurements[19,20] on a single crystal of the parent compound, $LaCoO_3$, showed that strong FM and weak antiferromagnetic (AFM) *dynamic* correlations develop and become randomized in all directions in support of a thermally activated transition to the IS state. The presence of both types of correlations is reminiscent of $LaMnO_3$ where static in-plane FM and out-of-plane AFM correlations are present. Concurrent neutron measurements reported in Ref. 21 on a powder sample concluded that the excited state is the HS state. Clearly, distinguishing one scenario from another in the doped compositions will not be easy also when mixing of Co^{3+} and Co^{4+} ions occurs. It is known that the FM correlations become static, while the AFM ones disappear with doping. At the same time, the system goes from an insulating to a metallic state. It is possible then to use the

insulating state where electrons are localized to identify the Co ions' orbital state: the partial occupancy of the e_g^1 orbitals in the $S=1$ state may lead to a structural deformation of the CoO_3 octahedra through a *Jahn-Teller* (JT) distortion. In comparison, the $S=2$ state is not orbitally active since the e_g orbital is fully occupied. The presence of magnetically induced JT polarons has been alluded to in other studies such as Refs. 14, 22, and 23 including our own neutron-diffraction measurements in compounds with A'=Sr,[8] and is important to understand the insulator-metal transition (IMT) and magnetoresistance mechanism in this class of materials. The stability of the $S=1$ state with hole doping is counterintuitive since it implies localization involving elastic energy as the lattice deforms around such magnetopolarons. The implications of such a mechanism need to be explored further as they are in stark contrast to the evolution of magnetopolarons with hole doping in manganites.[24]

The FM metallic state is reached by introducing hole carriers through the substitution of other divalent ions besides Sr such as Ca and Ba, but no information is available on the evolution and stability of the excited spin state with change in the electron hopping integral.[25–27] The ions of Ca, Sr and Ba have nominally different ionic sizes,[28] and the effective bandwidth changes in a way that can provide a measure of the role of the lattice via the ionic size effect.[29] Bandwidth control has been investigated earlier in the colossal magnetoresistive (CMR) manganites.[30] It has been found that JT polarons vanish with widening of the bandwidth, while the crystal transforms to a symmetry that is conducive to enhancing transport. In the manganites, a "flat" bandwidth leads to a rise in the IMT and FM transition temperatures T_C, while a narrow bandwidth leads to the reverse effect. It is generally presumed that for ions with small radius, i.e., Ca, charges become self-trapped and are more likely to form polaronic states that are localized by disorder while rendering the system insulating.[31] Thus, the degree of distortion is presumed higher in narrow bandwidth materials than in systems with expected broad bandwidths.[24] Little is known of these effects in cobaltites; thus these are the focus of the present paper. Such a study will provide useful insights into the effects of bandwidth on the formation of spin activated JT polarons or magnetopolarons as well as on the nature of the spin-lattice interactions.

TABLE I. The average A-site radii $\langle r_A \rangle$ and T_C are listed for Ca, Ba, and Sr samples at three concentrations. The A-site radius was determined using the ninefold-coordination value of the Co ion from Ref. 28. The value of T_C depends upon the definition applied as the transition temperature, as the transitions are quite broad. It was estimated by linearly extrapolating the upturn in magnetization to the x axis.

x	Cation	$\langle r_A \rangle$ (Å)	T_C (K)
0.1	Ca	1.212	55
	Sr	1.225	45
	Ba	1.241	110
0.2	Ca	1.209	145
	Sr	1.235	240
	Ba	1.267	186
0.3	Ca	1.205	150
	Sr	1.244	240
	Ba	1.292	205

Several unresolved issues regarding the nature of the Co electronic structure, the degree of Co to O hybridization, the strengths of Coulomb interactions, Hund's coupling, and the magnitude Δ of charge transfer energy prevail in spite of years of research in this field.[32] By carefully controlling the electron hopping integral through isovalent substitutions at the A' site using the cations of Ca, Sr, and Ba, we probe how the local lattice transforms in response to the change in the Co electronic structure. In addition, we investigate whether the bandwidth control is sufficient to explain the crossover to a metallic state or whether an unconventional JT mechanism may be more appropriate. To do so, we used pulsed neutron diffraction and the pair density function (PDF) analysis to determine the evolution of the local atomic structure, which clearly showed that the introduction of Co^{4+} ions stimulates the population of JT polarons, which increases rapidly above a critical radius of 1.22 Å in the insulating phase. Local JT distortions become static, costing the system significant elastic energy that must be compensated for by the stability of magnetic IS-LS exchange interactions. Below the IMT, the lattice softens and the static signature of the magnetopo-

larons disappears. This may involve dynamic IS-LS exchange interactions mediated by the double exchange between Co^{4+} and Co^{3+} ions.

Powder samples were prepared by standard solid-state reaction method. The concentration of x varied from 0% to 30% for Ca samples and from 0% to 50% for Ba and Sr samples. Table I lists the compositions, the average ninefold-coordinated ionic sizes $\langle r_A \rangle$, and the Curie transition temperatures for some of the samples studied to give a sense of how the average radius varies with x at the A site. The time-of-flight neutron experiments were performed at the NPDF of Los Alamos National Laboratory and at GLAD of Argonne National Laboratory. The samples were sealed in a vanadium can under helium atmosphere and placed in a closed-cycle refrigerator; measurements were performed as a function of temperature. The diffraction data were Fourier transformed in real space to obtain the local atomic PDF. The PDF represents the real-space correlations between atoms and is volume averaged and weighted by the neutron-scattering lengths. The magnetic and transport properties of all samples were characterized as well. In Fig. 1, the resistivities and magnetoresistances (MRs) as functions of field of two samples of Ca and Ba compressed into pellets with a concentration of $x=0.2$ are compared. In the case of Ca, an IMT is observed at ~ 145 K (Refs. 33 and 34) that coincides with T_C. In the case of Ba, although T_C is ~ 186 K as estimated from the bulk susceptibility measurements, the IMT is very broad and not so obvious while a very high residual resistivity is observed at very low temperatures, much higher than in the case of Ca. In both cases, the MR does not become "colossal," while in the Ca sample, a crossover from negative to positive values is observed. A negative MR peak appears around T_C that increases with field as expected due to increase in the sample's polarizability; a positive MR peak is observed around 50 K. In the case of Ba, the MR stays negative at all temperatures.

The local atomic structure in the vicinity of the Co-O octahedron evolves from the Mott insulating state of the parent compound, $LaCoO_3$, in the way shown in Fig. 2 for $x=0.2$ of Ca, Sr, and Ba. The radial distribution function (RDF), $4\pi r^2 \rho(r)$, plotted in the region corresponding to the Co-O bond distances is determined from diffraction data collected at 300 K with all samples in the paramagnetic and
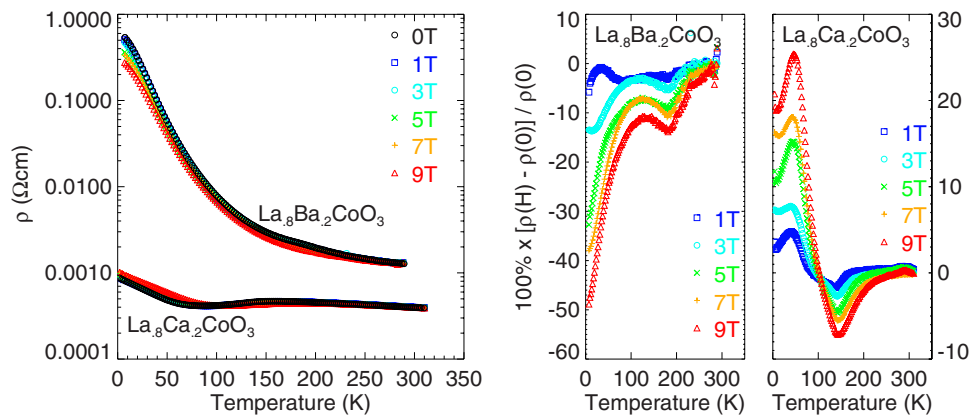

FIG. 1. (Color online) The temperature dependences of the resistivity and magnetoresistance as functions of magnetic field in $La_{0.8}Ca_{0.2}CoO_3$ and $La_{0.8}Ba_{0.2}CoO_3$. A crossover from negative to positive MR is observed around the IMT for the Ca sample but not for Ba.
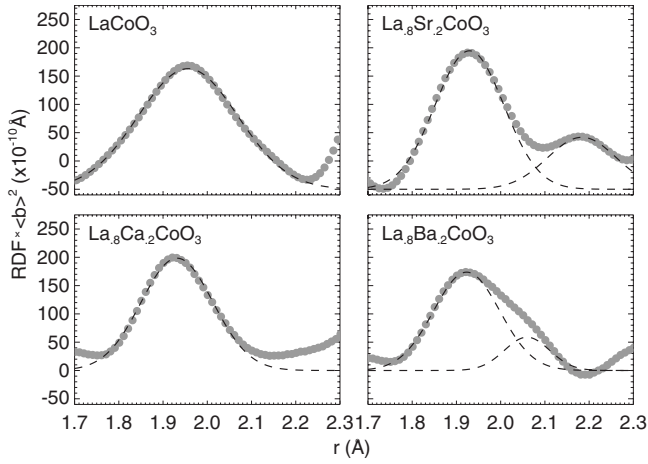
FIG. 2. The first peaks of the RDF corresponding to the shortest distance in the crystal structure multiplied by $\langle b \rangle^2$ for (a) $LaCoO_3$, (b) $La_{0.8}Ca_{0.2}CoO_3$, (c) $La_{0.8}Sr_{0.2}CoO_3$, and (d) $La_{0.8}Ba_{0.2}CoO_3$ are shown for data collected at room temperature.

FIG. 3. The percentage of JT sites as a function of the average ionic radius at the *A* site determined from data collected at $T = 300$ K. No magnetopolarons can be assumed below the critical radius of $\langle r_c \rangle = 1.22$ Å. Magnetopolaron formation appears to saturate above $\langle r_A \rangle = 1.28$ Å. Data for 30% compositions for all samples were omitted because of reasons described in some detail in previous work such as the one in Ref. 8. The type of ion and concentration is indicated on each point.

insulating state. The RDF is multiplied by $\langle b \rangle^2$, where $\langle b \rangle$ is the compositionally averaged neutron-scattering length, so that the intensity of the Co-O peak can be directly compared in each composition. In (a), $LaCoO_3$ shows no clear signature of static JT distortions. However, the Co-O bond peak is quite broad and clearly asymmetric. Although it is normal for the PDF peaks to become wider with increasing temperature due to increase in the atomic thermal motion, the asymmetry of this peak cannot be accounted for by such a thermal effect. In (b), the Co-O peak in $La_{0.8}Ca_{0.2}CoO_3$ is narrow and shows no asymmetry. Even though the crystal structure in Ca transforms to an orthorhombic symmetry (*Pnma*) from the rhombohedral $R\bar{3}c$,[35] this transformation is not associated with the formation of JT distortions. However, in (c) and (d), the Co-O peak shows a clear and strong split in Sr and Ba samples. This split can only be attributed as a consequence of the presence of JT distorted octahedra. The Co-O peak has been fitted by two Gaussian curves. Two assertions can be made from the double Gaussian curve fitting: one is that it offers strong evidence for the presence of local and static JT distortions even though the symmetry remains rhombohedral; the other is that such distortions are created even as the presumed bandwidth becomes wider with Sr and Ba.

The formation of static JT is a consequence of stable magnetic IS states and such Co-O sites are hereby referred to as JT magnetopolarons. The number of magnetopolaron sites varies with the average ionic radius in the way shown in Fig. 3. This was determined from data collected at 300 K, in which case all the samples are insulating and paramagnetic. Thus, there is no double exchange between the Co ions that would enable hole hopping among the six neighbors. The nominal hole concentration is indicated for each sample. The percentage of Co-O sites that are elongated is estimated from the two Gaussian fittings and from setting the total area under the short and long bond peaks to 6, the coordination number in an octahedral environment. In the absence of JT, all Co-O bonds are symmetric and short, and the area under the peak corresponds to the coordination. However, in the presence of JT and with the $d_{z^2-r^2}$ orbital occupied, the Co-O
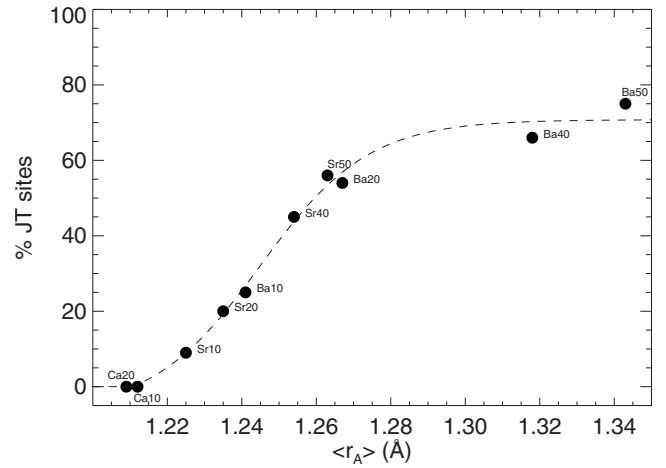
bonds split to 4 short and 2 long for a total of 6. Thus, as the area under the short Co-O peak starts to deviate from the coordination of 6 (0% JT) to 4 (100% JT), long Co-O bonds appear. As seen in Fig. 3, when the ionic radius exceeds the critical value of $\langle r_c \rangle = 1.22$ Å, the percentage of JT sites starts to rise and reaches a value close to 80% with only 50% of Ba doping. It appears to saturate around $\langle r_A \rangle = 1.28$ Å. JT distorted sites are not evident in Ca containing materials at this temperature but are clearly present in Sr and Ba samples. In Sr containing samples, for each hole, there is one JT site created. However, for the case with Ba doping, for each hole there are about three JT sites created up to 20%. For higher concentrations, the number of JT sites created per hole drops to about 1.5 per hole. The formation of the JT magnetopolarons must involve a substantial lattice energy in the paramagnetic and insulating state.

The Co-O-Co bond angle changes with the average ionic radius at the rare-earth site in the way shown in Fig. 4. For values of $\langle r_A \rangle < 1.22$ Å, the bond angle does not change much with x. For values of $\langle r_A \rangle > 1.22$ Å, the angle increases linearly with $\langle r_A \rangle$ and approaches 180°. Decreasing $\langle r_A \rangle$ bends the Co-O-Co bond angle in addition to reducing the electron hopping and consequently the bandwidth. This is the case of Ca-doped samples, where the symmetry changes from rhombohedral to orthorhombic as was previously observed[34,35] at $x \sim 0.1$. The bond is significantly bent with Ca even with only 10% of doping. This suggests that the small size of Ca distorts the local environment in such a way that the octahedra rotate toward the smaller ion. The environment around Ca most likely allows for FM coupling between spins where charges are not localized on specific Co sites but can be shared within the extended distorted region. We have previously seen that ferromagnetism saturates for Ca by 20% and the reason for this might be that it never truly becomes an itinerant FM state. Such a distorted environment
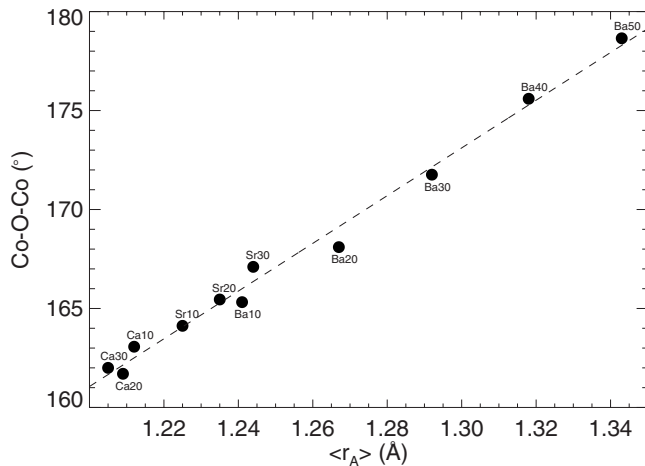
FIG. 4. The Co-O-Co bond angle as a function of $\langle r_A \rangle$. The Co-O-Co bond is severely bent below 1.22 Å, which corresponds to Ca compositions, but unbends for higher values. The type of ion and its concentration are indicated on each point.

may be the reason as to why T_C does not rise above 150 K in Ca. However, in Sr- and Ba-doped samples, the crystal symmetry remains rhombohedral but the tilting is reduced, approaching a cubic structure. The bond angle continuously unbends, while the number of JT sites increases simultaneously. Below the magnetic transition, the local atomic structure shows no evidence for the long Co-O bonds in any of the samples.

The bent octahedra of the orthorhombic Ca structure come about with hole doping. This indicates that the orthorhombic symmetry creates an environment around each Ca ion in such a way that the hole can hop from site to site and does not remain long enough on one site to create a static JT distortion. On the other hand, in Ba- and Sr-doped samples, the hole is localized long enough that static (at the time scale of the neutron experiment) are created. Why are the Ba and Sr systems more likely to exhibit JT distortions? The increased tendency might be due to phase separation. Using single crystals, we have observed the presence of two magnetic entities, one commensurate and another that is incommensurate with the lattice, with different onset temperatures.[34] The incommensurate phase has been well established in Sr and Ba crystals but is absent in Ca crystals.[34,36] Above the magnetic transition, the phase is paramagnetic and spin disorder localizes the hole to one (as in the case of Sr) or more (approximately three in the case of Ba) sites. These JT magnetopolarons could be formed in close proximity to the dopant, but there is no indication of ordering above the transition. Below the magnetic transition, the majority phase has ferro-ordering. JT distortions are no longer observed. This suggests that the charges are no longer localized per site but become mobile. At the same time, in this temperature regime, the two magnetic phases appear. Clearly, the majority phase (FM) carries most of the carriers as the system becomes metallic. But some carriers are most likely trapped in what gives rise to the incommensurate phase.

In summary, the average crystal structure remains largely unchanged with Sr and Ba additions. But with increasing Ca, it transforms to orthorhombic, where the Co-O-Co bond is significantly bent. With x up to 0.3, no JT polarons are evident in spite of the high charge content, which suggests that the lattice may play a more important role in the formation of JT magnetopolarons. Formation of JT magnetopolarons with increase in x and with widening of the bandwidth must be accompanied by a long-range stress field. As the temperature is lowered and spin fluctuations decrease, the spins align ferromagnetically and allow itinerant electrons to gain kinetic energy. Transport is via hopping of $Co^{3+} \rightarrow Co^{4+}$ ions. In doing so, a hole needs to displace ions in the $S=1$ state, which is associated with a large JT coupling. This most likely arises from the manifestation of strong electron-phonon coupling. Phonons have been previously observed to change with both temperature and doping.[8] This requires that the large elastic energy present around the polaron in the paramagnetic (PM) phase be released with the transition as no polarons are evident below T_C. In conclusion, we have shown that straight Co-O-Co bonds are conducive to creating JT magnetopolarons, while buckling of the bond leads to no JT and no IS states. Bond bending has also been associated with the suppression of superconductivity in cuprates, which takes place to release the strain associated with stripe formation.

*Present address: NIST Center for Neutron Research, Gaithersburg, MD 20899.

[1] M. Rini, R. Tobey, N. Dean, J. Itatani, Y. Tomioka, Y. Tokura, R. W. Schoenlein, and A. Cavalleri, Nature (London) **449**, 72 (2007).

[2] M. Coey, Nature (London) **430**, 155 (2004).

[3] E. Dagotto, Science **309**, 257 (2005).

[4] G. C. Milward, M. J. Calderon, and P. B. Littlewood, Nature (London) **433**, 607 (2005).

[5] T. Hotta, A. Feiguin, and E. Dagotto, Phys. Rev. Lett. **86**, 4922 (2001).

[6] J. Q. Li, M. Uehara, C. Tsuruta, Y. Matsui, and Z. X. Zhao, Phys. Rev. Lett. **82**, 2386 (1999).

[7] P. G. Radaelli, G. Iannone, D. E. Cox, H. Marezio, H. Y. Hwang, and S. W. Cheong, Physica B **241**, 295 (1997).

[8] D. Louca and J. L. Sarrao, Phys. Rev. Lett. **91**, 155501 (2003).

[9] P. M. Raccah and J. B. Goodenough, Phys. Rev. **155**, 932 (1967).

[10] D. Louca, J. L. Sarrao, J. D. Thompson, H. Röder, and G. H. Kwei, Phys. Rev. B **60**, 10378 (1999).

[11] Y. Kobayashi, N. Fujiwara, S. Murata, K. Asai, and H. Yasuoka, Physica B **281**, 512 (2000).

[12] A. Ishikawa, J. Nohara, and S. Sugai, Phys. Rev. Lett. **93**, 136401 (2004).

[13] T. Saitoh, T. Mizokawa, A. Fujimori, M. Abbate, Y. Takeda, and M. Takano, Phys. Rev. B **55**, 4257 (1997).

[14] S. Yamaguchi, Y. Okimoto, and Y. Tokura, Phys. Rev. B **55**, R8666 (1997).

[15] G. Maris, Y. Ren, V. Volotchaev, C. Zobel, T. Lorenz, and T. T. M. Palstra, Phys. Rev. B **67**, 224423 (2003).

[16] C. Zener, Phys. Rev. **81**, 440 (1951).

[17] M. A. Señaris-Rodriguez and J. B. Goodenough, J. Solid State Chem. **118**, 323 (1995).

[18] P. L. Kuhns, M. J. R. Hoch, W. G. Moulton, A. P. Reyes, J. Wu, and C. Leighton, Phys. Rev. Lett. **91**, 127202 (2003).

[19] D. Phelan, Despina Louca, S. Rosenkranz, S.-H. Lee, Y. Qiu, P. J. Chupas, R. Osborn, H. Zheng, J. F. Mitchell, J. R. D. Copley, J. L. Sarrao, and Y. Moritomo, Phys. Rev. Lett. **96**, 027201 (2006).

[20] D. Phelan, Despina Louca, K. Kamazawa, M. F. Hundley, and K. Yamada, Phys. Rev. B **76**, 104111 (2007).

[21] A. Podlesnyak, S. Streule, J. Mesot, M. Medarde, E. Pomjakushina, K. Conder, A. Tanaka, M. W. Haverkort, and D. I. Khomskii, Phys. Rev. Lett. **97**, 247208 (2006).

[22] S. Yamaguchi, Y. Okimoto, H. Taniguchi, and Y. Tokura, Phys. Rev. B **53**, R2926 (1996).

[23] S. Yamaguchi, Y. Okimoto, K. Ishibashi, and Y. Tokura, Phys. Rev. B **58**, 6862 (1998).

[24] D. Louca, T. Egami, E. L. Brosha, H. Röder, and A. R. Bishop, Phys. Rev. B **56**, R8475 (1997).

[25] T. Takami, J.-S. Zhou, J. B. Goodenough, and H. Ikuta, Phys. Rev. B **76**, 144116 (2007).

[26] S. Yamaguchi, Y. Okimoto, and Y. Tokura, Phys. Rev. B **54**, R11022 (1996).

[27] J.-Q. Yan, J.-S. Zhou, and J. B. Goodenough, Phys. Rev. B **69**, 134409 (2004).

[28] R. D. Shannon, Acta Crystallogr., Sect. A: Cryst. Phys., Diffr., Theor. Gen. Crystallogr. **32**, 751 (1976).

[29] T. Egami and Despina Louca, Phys. Rev. B **65**, 094422 (2002).

[30] H. Y. Hwang, S.-W. Cheong, P. G. Radaelli, M. Marezio, and B. Batlogg, Phys. Rev. Lett. **75**, 914 (1995).

[31] M. Jaime, H. T. Hardner, M. B. Salamon, M. Rubinstein, P. Dorsey, and D. Emin, Phys. Rev. Lett. **78**, 951 (1997).

[32] D. Louca, T. Egami, W. Dmowski, and J. F. Mitchell, Phys. Rev. B **64**, 180403 (2001).

[33] M. Kriener, C. Zobel, A. Reichl, J. Baier, M. Cwik, K. Berggold, H. Kierspel, O. Zabara, A. Freimuth, and T. Lorenz, Phys. Rev. B **69**, 094417 (2004).

[34] D. Phelan, D. Louca, K. Kamazawa, S.-H. Lee, S. Rosenkranz, M. F. Hundley, J. F. Mitchell, Y. Motome, S. N. Ancona, and Y. Moritomo, Phys. Rev. Lett. **97**, 235501 (2006).

[35] J. C. Burley, J. F. Mitchell, and S. Short, Phys. Rev. B **69**, 054401 (2004).

[36] J. Yu, D. Louca, K. Yamada, and D. Phelan (unpublished).